Visualizing motions of magnetic fluid spikes for a novel particle-collecting device

doi: 10.1007/s12650-018-0504-4

Satoshi Uehara, Misaki Kiuchi, Hideya Nishiyama

Visualizing motions of magnetic fluid spikes for a novel particle collecting device

Abstract This paper proposes a novel method to collect fine and coarse particles dispersed in the air using magnetic fluid to improve atmospheric environment. Magnetic fluids are set in the 50 × 50 × 10 mm rectangular channel. Plain flour particles ranging from 2.5 μm to 450 μm were used as model particles. Then, filtration efficiency of 40 % is obtained as a maximum value. We propose a unique method to visualize and quantitatively evaluate the interaction between wind and magnetic fluid which found to be an important factor for enhance the particle collecting efficiency. Generally, it is difficult to measure the magnetic fluid flow since it is not transparent against light. In our developed method, we use LED light sheet which is low cost unlike lasers. Furthermore, no need to add anything into the magnetic liquid and no need to dilute the liquid. It is found that the spikes are flown by the stream depending on the magnetic field strength.

Keyword Magnetic fluid · Flow visualization·· Particle collection · Environmental cleaning · Liquid interface

1 Introduction

Economic growth has increased atmospheric aerosol concentrations dramatically in recent decades. Fine and coarse particles from factory, car and construction site harm human health. Under the governmental regulations, particle collecting technologies has been drastically developed in this several decade to improve the atmospheric situations (Niewulis, Podliński, & Mizeraczyk, 2009; Zouzou, Dramane, Moreau, & Touchard, 2011).

For instance, DPF (Diesel Particulate Filter) on vehicles can remove the emission of fine pollutant particles from the combustion inside an engine. Also, fibrous filter is commonly used to remove particles. It is possible to remove more than 99.97 % of particle with a size of 0.3 μm using HEPA (High efficiency particulate air) filter. Particles are deposited on the filter made of thin fibers by inertial impactions interceptions, diffusions and sieving of particles(Dunn & Renken, 1987). The filter pores are small enough to achieve the high efficiency for fine-particle collection. Therefore, a pre-filter which made of polymer or glass wool for relatively coarse-particle collection is set in upper stream to avoid the HEPA filter from clogging (Japuntich, Stenhouse, & Liu, 1994; Silva, Negrini, Aguiar, & Coury, 1999; Song, Park, & Lee, 2006; Thomas, Penicot, Contal, Leclerc, & Vendel, 2001). Especially when the gas includes a large amount of dust, it must be necessary to set a pre-filter to extend the life limit of a HEPA filter. Furthermore, when a used filter is replaced with a new one, whole system should be stopped so that extension of replacement cycle is required

With considering these background, we propose a noble particle - filtering method using magnetic fluid spikes which can use as pre-filter. A magnetic fluid consists of a suspension of nano-sized iron particles in a carrier liquid such as water, mineral oil, or kerosene. The application of a magnetic field results in the formation of spike-like shapes under gravity, due to the counterbalancing effect of gravitational force, the magnetic force and surface tension(Uehara, Itoga, & Nishiyama, 2015; Zahn, 2001).

The merit of using magnetic fluid is that a magnetic fluid exists in a liquid state under a room temperature although the surface forms a spike-like shape. Liquid has a high filtration character against a particle. For instance, there is a method to remove particles from gas by using collision with liquid surface such as wet scrubber. In the method, particles are collected by the collision with a liquid droplet generated by liquid spray. Dust particles are removed as a liquid, then cleaner gas is ejected. In our developed device, the main part of particle collecting system is made of magnetic fluid. Magnetic fluid has not only high filtration efficiency but also high controllability since it can be moved by a magnetic field. Furthermore, using permanent magnet to generate a magnetic field consume less energy. The magnetic spikes can generate even in a small space as long as a magnetic field exists. Generally, the

minimum size of single magnetic spike is several mm height and diameter. Therefore, there is a size limitation of our proposed device. However, the advantages are the convenience of forming the spikes. It is also expected to remove the magnetic fluid after a filtration easily by controlling a magnetic field.

First, we develop a fundamental experimental setup for measuring an filtration efficiency by magnetic fluid spikes. During the observations, interesting phenomena of magnetic-fluid-spike's motion by applying a gas was observed. It is considered that the magnetic-fluid-spike's flow plays an important role for enhancing a collection efficiency. Hence, second part of the paper, we propose a new method to observe magnetic-fluid-spike's motion and show quantitative results with various magnetic field strength.

Magnetic fluid rheology and its flow have gathered many attentions (Rinaldi, Chaves, Elborai, He, & Zahn, 2005). The velocity measurement using ultrasonic Doppler method was conducted with adding tracer particle (Kikura, Takeda, & Sawada, 1999). Also, spike motions by variation of magnetic fields have reported (Promislow & Gast, 1996; Sudo, Asano, Takana, & Nishiyama, 2011). Furthermore, from the view point of the application for drag targeting, a magnetic fluid in a liquid flow has been investigated (Voltairas, Fotiadis, & Michalis, 2002)(Ruuge & Rusetski, 1993). For instance, Ganguly et al. reported a diffusion of the magnetic fluid into a host liquid (Ganguly, Gaind, Sen, & Puri, 2005).

However, spike's flow caused by air flow has not been studied much. Especially, there are quite less studies on focusing the spike-like interface motion. The main reason is a difficulty of observation of a magnetic fluid. Magnetic fluid is a black colored liquid. PIV (Particle Image velocimetry) method cannot be applied to since a laser light cannot penetrates into a magnetic fluid. Furthermore, oil-based magnetic fluid reflect a light on the surface. In our proposing method, this reflectability is used for detecting the position of magnetic fluid spikes.

We successfully measured the spike motion under the applying wind. A spike fluidity is different depending on a position. It is found that higher magnetic field realize a low mobility of the spikes. This study shines a light on the unique property of magnetic fluid which is a spike-like interface shape although it has not been paid much attention as practical applications previously.

2 Experimental setup

Figure 1 shows the schematic of the concept and the experimental setup for measuring an amount of adsorbed particles. In our proposed method, magnetic fluid act as a pillar like filter. Adsorbed part which consists of rectangular channel, magnetic fluid and Neodymium magnet is set on the electric scale. The channel is made of acrylic plate. The size of the channel and Neodymium magnet are 40 × 250 × 10 mm and 50 × 50 × 10 mm, respectively. The surface magnetic flux density of the Neodymium magnet is 211 mT. Air containing model particles is passing through the channel. Total amount of particles which adsorbed on the magnetic fluid surface is measured by the electric scale with evolution of time. The distance in between the bottom of magnetic fluid and Neodymium magnet can be controlled by using a microstage.

The characteristic height of spikes is several mm which is smaller than the channel height (The

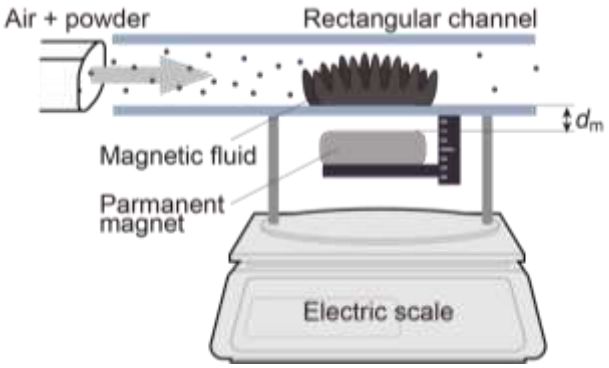

Fig. 1 Experimental setup for particle collection measurement by using electric scale.

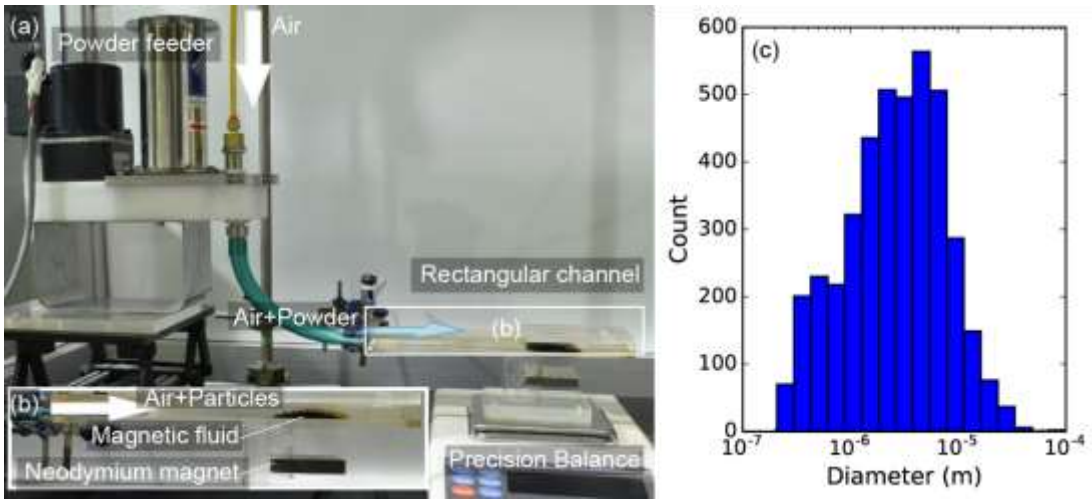

Fig. 2 Photos for experimental setup. (a) Whole setup and (b) particle collection part. (c) Size distribution of model particles.

height is shown in Section 3.2 in detail). The height of the spike is variable with the magnetic field strength. In our experiment, channel height is higher than the spike to prevent the spikes touching to the upper channel wall in order to obtain a fundamental data with maintaining the magnetic fluid spike shape. Therefore, in our experiment, in the vicinity of the upper channel wall, there exist particles which pass through the filtering part without interference with the magnetic fluid spikes.

Figure 2 (a) and (b) shows the whole image and zoomed image of experimental setup. 25 NL/min air passing through the powder feeder is introduced into the rectangular channel with containing model particles of Q = 110 mg/s. Plain flour was used as model particles since it is easy and safe to use. Median diameter of the plain flour particles, D_{50}, was 3.2 μm, although a size distribution of the particles was about 2.5 μm – 450 μm. A target in this study is coarse powder which should be removed by pre-filter before introducing into a main HEPA filter. Therefore, plain flour which has such a size distribution is suit for our experiment. The size distribution of the particles is shown in Fig.2 (c). To avoid an interruption of the flow, outlet of the channel is open to the atmosphere. Therefore, we do not obtain the data about the particles after passing the device. This insists that the particle size dependence on the collecting efficiency is unknown.

Generally, a traceability of fine particle is defined by a Stokes' number. The particle tends not to follow a stream line as the size is large. It is considered the larger particles are filtered than the small one. In the particle collecting experiment, Neodymium magnetic holder made from acrylic pipe is used instead of microstage since the weight of microstage is much heavy for the precision balance. With using the magnet holder, magnet position can be varied as d_m = 10, 25 and 40 mm. The magnetic strength on the bottom of the channel corresponding to the magnet positions are 151, 70 and 33 mT, respectively.

3 Results and discussion

3.1 Characteristics of particle filtration

Figure 3 (a) shows the time evolution of particle filtration amounts, $M(t)$, with changing a magnetic field strength. The graphs are monotonically increasing with time. This graph indicates the increasing of the weight in the rectangular channel due to the particle filtration. Note that, during the experiment, adsorbed particles were observed on the inner wall of the rectangular channel. Therefore, the experimental data includes an effect of not only the magnetic fluid but also the acrylic inner surface of the channel.

In the Fig. 3 (a), the graphs are discontinuous in some point. This is because the aggregated particles are introduced into the channel occasionally. To ignore these data and investigate a time

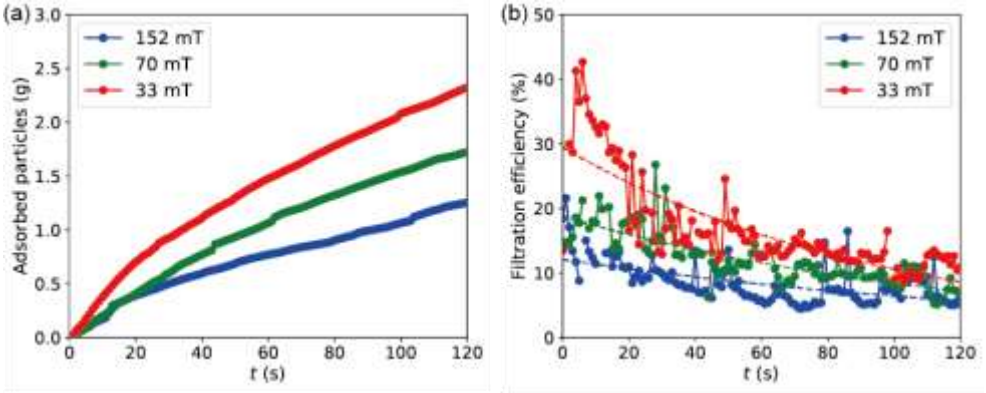

Fig. 3 (a) Amount of adsorbed particles. (b) Filtration efficiency.

depending particle filtration, filtration efficiency per unit time is obtained from data of Fig. 3 (a). An amount of particle filtration per second, C, is obtained by the Eq. (1). The effect of unexpected particle inflow was removed by using moving average, $\bar{c}_i$ as shown in Eq. (2) and (3). Then, filtration efficiency was derived by devideng C by introducing amount of particles Q. The result is shown in Fig. 3(b).

$$C = \frac{M(t+\Delta t) - M(t)}{Q\Delta t}. \tag{1}$$

$$\bar{c}_i = \frac{1}{N}\sum_{i=k}^{k+N} c_i \quad . \tag{2}$$

$$C = \{c_i |\ c_i < c_{error} + \bar{c}_i\} \quad . \tag{3}$$

Here, N is 5 and c_{error} is 0.01 g. Dashed lines in the graph show fitting with the exponential curve of $y = b \exp(-at)$, where a and b are fitting parameters. As shown in the graph in the case of 33 mT indicates a highest filtration efficiency in our experiment. Obviously, there required a minimum value of magnetic field to maintain the spike shape, however, lower magnetic field indicates better particle collecting efficiency. The reason of this magnetic field dependence is discussed in next section 3.2.

The filtration efficiency decreases with evolution of time. The reason is related to the changing of the magnetic fluid property. While conducting a particle collecting experiment, adhesion of particles decreases viscosity of the magnetic fluid. The fact reduces mobility of the magnetic fluid spikes. In 120 s of the experiment, magnetic fluid spikes stop to flow and behave like a solid object. If a solid object is placed in a flow, stream lines avoid the object. In this case, particles flow on a stream line with avoiding the solid like magnetic fluid. However, particles still occasionally collide on the magnetic fluid surface by Brownian motion and turbulence of the flow, so that the filtration efficiency decreases to extremely small but not to zero.

3.2 Visualization of the magnetic spike mobility

Visualization and optical measurement are important to clarify physical phenomena. In this section, we focus on observing the motions of magnetic fluid spikes. The characteristics of the spike's motion qualitatively.

First, cross sectional view of magnetic spikes with various magnetic strength is shown in Figure 4. Magnetic strength is controlled by changing the position of permanent magnet from the channel bottom by using the microstage. Note that, we use a permanent magnet to generate a magnetic field for low energy consuming application. Therefore, magnetic lines of force are not constant in these experimental conditions. Magnetic fluid forms a spike-like shape on the interface. This phenomena

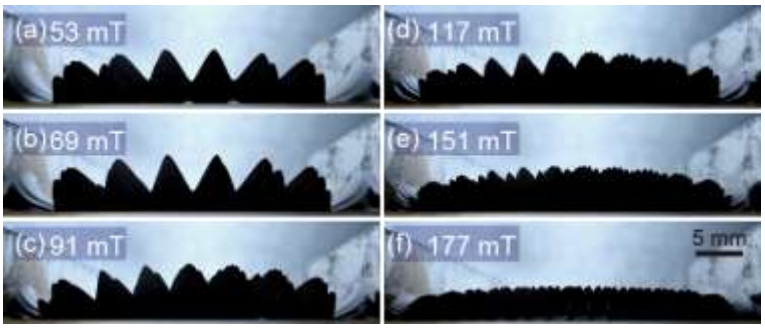

Fig. 4 Cross sectional photos of magnetic fluid spikes with various magnetic fields.

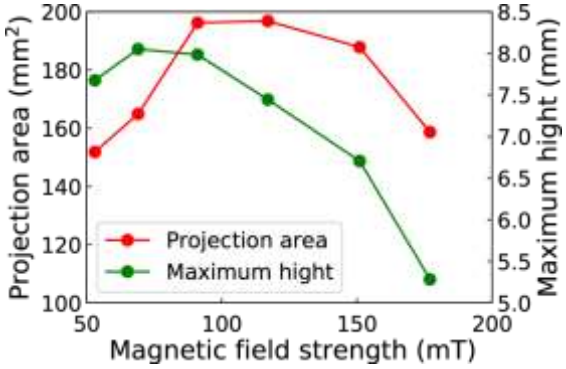

Fig. 5 Projection area and maximum height of magnetic fluid spikes with various magnetic field strength.

referred to as a Rosensweig instability which is first studied by Cowley and Rosensweig (Cowley & Rosensweig, 1967). If a uniform and vertical magnetic field is applied on a magnetic fluid, a pattern of peaks emerge on the surface when the field strength is above a critical value. That causes a local bunching of magnetic field lines. Magnetic fluid is attracted to the strong-field region, amplifying the perturbation and further increasing of field gradient.

Figure 5 shows the height and projection area of the magnetic fluid spikes as shown in Fig. 4. The height is measured as a distance from channel bottom to the highest spike tip. The projection areas are obtained by binarizing the images in Fig.4. The spikes grow with increasing a magnetic strength. However, over around 70 mT, higher magnetic strength realizes stronger magnetic dipolar coupling. Each iron particles in magnetic fluid are attracted to the bottom of the channel. Each spikes cannot maintain the high spike shape and transitions to multiple small spikes (Fig.4 (f)). Then, a number of spikes with lower height increases due to the balance of surface tension, gravity and magnetic force. On the other hand, projected area increases until around 120 mT due to the increase of the number of the spikes.

The height and projection area affect the characteristics of particle collection efficiencies since the flow collide on the front edge of a magnetic fluid. However, the tendency of Fig.5 is in disagreement with the one in Fig. 3. Furthermore, when we observed the magnetic spikes during the particle collecting experiment, we found that the spikes are moving along the wind. Hence, the static characteristics is not considered as a main factor of the magnetic field dependence on the particle collection characteristics.

As mentioned above, magnetic fluid under a magnetic field generate spike shape with keeping a liquid property. Therefore, when the wind is introduced into a channel, then magnetic fluid spikes changes their positions. The mobility of the spike motions, in other words, the fluidity, is related to the physical property of the magnetic fluid. As described in Fig.3 (b), the fluidity is important the filtration efficiency.

From these results, we set up a hypothesis that fluidity is different with magnetic field since the apparent viscosity of a magnetic fluid changes with a magnetic field strength and the fluidity affects

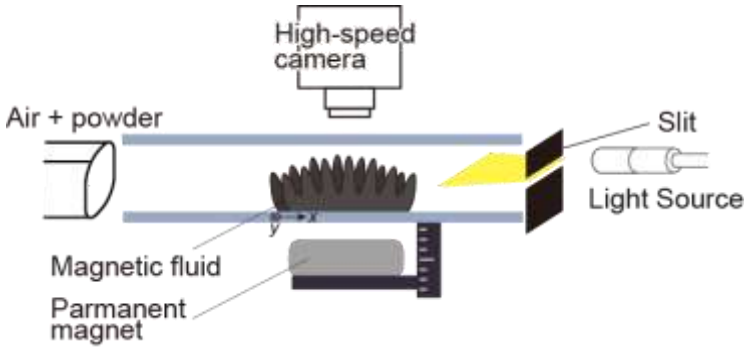

Fig. 6 Visualization method for the magnetic-fluid-spike tips.

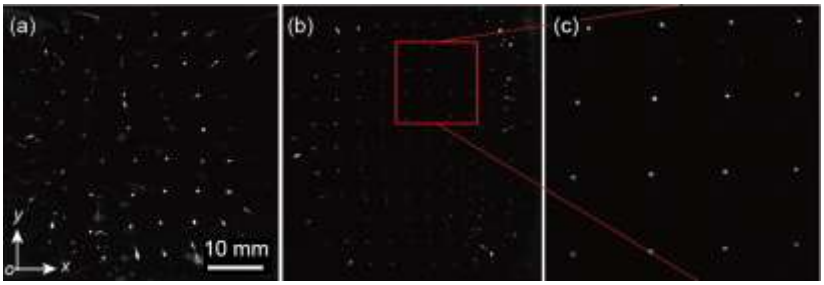

Fig. 7 Visualized image of magnetic-fluid-spike tips under the magnetic field of (a) 69 mT and (b) 117 mT. (c) Zoomed image of red lined rectangular area in (b).

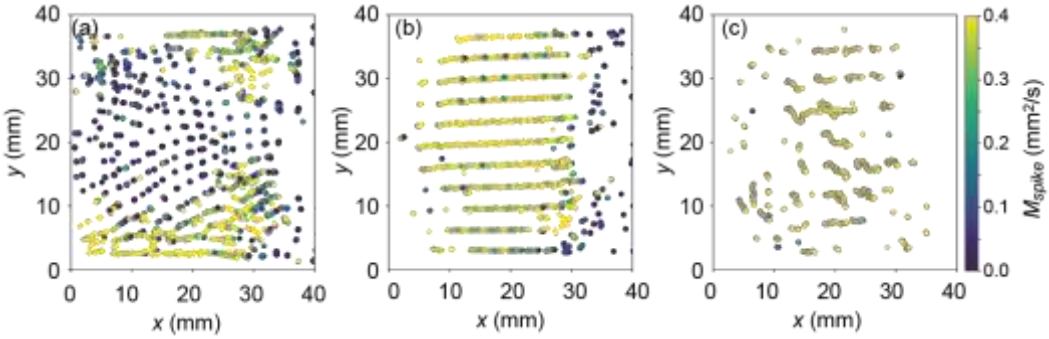

Fig. 8 Visualization of spike tip's motion under the magnetic field of (a) 177 mT, (b) 117 mT and (c) 69 mT. The color of symbols indicate the mobility.

the particle collection efficiency. The rest of this paper, we describe a novel method to visualize motions of magnetic fluid spikes and we show the results of the quantitative analysis. It is difficult to conduct optical observation since a magnetic fluid is a black colored liquid. PIV (Particle Image velocimetry) method cannot be applied to since a laser light cannot penetrates into a magnetic fluid. Furthermore, oil-based magnetic fluid reflect a light on the surface. In our proposing method, this light-reflecting property is utilized for a visualization and detection of a spike positions.

Figure 6 shows the schematic of our developed method. LED light focused by lens is inserted into the channel through a slit with the width of 3 mm. The light sheet has 3 – 6 mm thickness unlike a very thin laser sheet. When the light hit the spikes, in theory, the light is reflected toward the whole direction of the upper hemisphere at the tip of a spike. On the other hand, the side surface of a magnetic spike does not reflect a light in the upward direction. Therefore, with setting a high-speed camera vertically above the cannel, only spike tips are observed as shown in Fig.7. Each bright spots in the picture indicate the tips of the spikes. Since the size of bright spot is small in Fig.7 (b), zoomed image of the red-lined rectangular area in Fig.7 (b) is shown in Fig.7 (c). Compared Fig.7 (a) with Fig.7 (b), it is observed that number of spikes are increased with the increasing of magnetic field strength. The size of the spot indicates the sharpness of a spike. Therefore, the spikes in Fig.7 (b) is much sharper

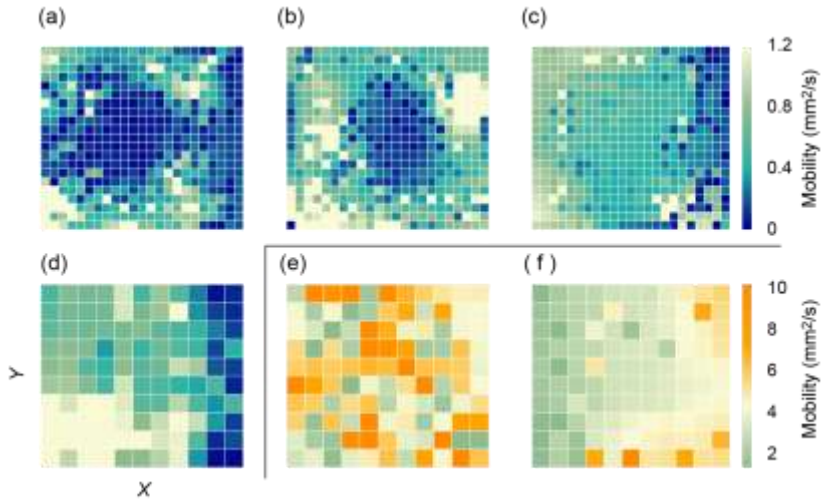

Fig. 9 Visualization of the magnetic-fluid-spike mobility with various magnetic field of (a) 177 mT, (b) 151 mT, (c) 117 mT, (d) 91 mT, (e) 69 mT and (f) 53 mT.

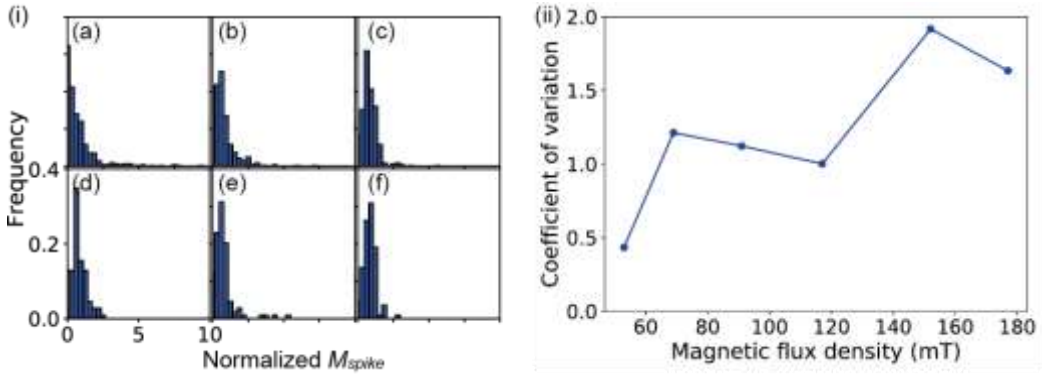

Fig. 10 (i) Histograms of M_{spike} under various magnetic field and (ii) coefficient of variation under

than the one in Fig.7 (a). These facts are in a good agreement with the cross sectional photo in Fig. 4. At the end, by tracking the bright spots, spike motions are analyzed.

Figure 8 shows the positions of spikes at each recorded frame in whole recording time. The color of the symbol indicates a mobility of each spikes. Here, we introduce a variable M_{spike} which define the tendency of spike motion by following equation.

$$M_{spike} = \frac{\langle x^2 \rangle}{dt}, \tag{4}$$

where, *dt* and *x* denote a time difference in between two images and displacement of the bright spot, respectively. This is based on the equation to obtain a diffusion constant of Brownian motion. Note that, the motions of spikes are not caused by Brownian motion, obviously. A spike tip not only moves toward the flow direction but also oscillates in the two dimensional plane which looks randomly. Therefore, we adopt M_{spike} to evaluate the fluidity of the spikes. The unit of M_{spike} is m^2/s. In the graph, brighter symbol indicates a larger value of M_{spike} , that is to say spike motion is active. The direction of the wind is from left to right in Fig. 7. That is corresponding to the positive direction of the *x* axis in Fig. 8. In the case of Fig.8 (b) and (c), the spikes in entire area moves along the wind. On the other hand, the spikes slightly move at the center of the area in the case of Fig.8 (a), for instance.

The plots shown in Fig.8 is corresponding to the so-called Lagrangian description. Here, we focus on a mobility with depending of the position of the spikes. Therefore, the results are transformed to the Eulerian description by obtaining the mean value in the arbitral area with using the Eq. (5). Observed area is divided into rectangle areas. Mean value, $\bar{M}_{spike}$ of M_{spike} in the each divided

rectangular areas is derived as below,

$$\bar{M}_{spike}(X,Y) = \frac{1}{N}\Sigma_{A} M_{spike}(x,y) \quad . \tag{5}$$

Where X and Y denote a position of the rectangular area. Then, finally, we visualized the mobility of spikes with depending on the magnetic field is shown in Fig. 9. N denotes a number of plots existing in the area.

Brighter area indicates that spike motion is active. The spike tips do not move actively in the dark area. From Fig. 9, it is found that when the magnetic field is strong, magnetic fluid spikes at the center part tend to have small mobility since the magnetic dipole-dipole interaction applied to the magnetic particles in the magnetic fluid is strong. On the other hand, when the magnetic field is weak, whole spikes are moves relatively uniform. In the case of weakest magnetic field, the motions of magnetic spikes are extremely large (Fig.9 (e) and (f)). As the end of this section, the difference described above is evaluated qualitatively as below.

Figure 10 (a) shows the histogram of normalized M_{spike} with various magnetic field conditions. A coefficient of variation which obtained from standard deviation divided by the average of M_{spike} at each condition is shown in Fig.10 (b). The coefficient of variation tends to increase with magnetic fluid strength. Therefore, the lower magnetic strength is, the more uniform spike motion is. The trend is in the agreement with the powder collecting efficiency which has the negative correlation with magnetic field strength at initial state. The visualized results here are obtained by using the wind which exclude particles. Practically, when the wind includes particles, the mobility would decrease as particles are deposited as discussed in Fig.3.

The results show that magnetic-fluid-spike's mobility can be controlled by changing a magnetic field strength. The fact is useful to control the device property such as a particle collection efficiency. Furthermore, filtering method has a problem that a filter becomes a flow resistance in a duct. Hence, our device has a possibility of changing the flow resistance by changing a spike shape controlled by magnetic field.

4 Conclusions

We developed a novel method to collect fine and coarse particles dispersed in the air using magnetic fluid to improve atmospheric environment. The main findings in the present study are summarized as follows.

(1) The particle filtration amount by using magnetic fluid spikes was measured. The dependence of magnetic field on the particle collection efficiency was clarified. When the magnetic field strength is smallest in our experiment, the device shows the highest particle collection efficiency as 46.9 mg/s.
(2) We developed the optical observation method for magnetic fluid spike motions by utilizing a light reflection property of magnetic fluid. The positions of the magnetic fluid spikes are successfully detected by using LED light source. The method is useful from the view point of a cost since an expensive Laser light source is not required.
(3) The magnetic fluid spike mobility caused by a surround wind was visualized with various magnetic field strength. It was found that the magnetic spike motion is different depending on the positions. When the magnetic field is relatively strong, the spike tips tend to move inactively at the center part. On the other hand, decreasing of the magnetic field strength makes the motions uniform.

Acknowledgment

This work was supported by JSPS KAKENHI Grant Number 16K14151. We would like to thank Mr. T. Nakajima for technical supports.

References

Cowley, M. D., & Rosensweig, R. E. (1967). The interfacial stability of a ferromagnetic fluid. *Journal of*

Fluid Mechanics, *30*(4), 671–688. https://doi.org/10.1017/S0022112067001697

Dunn, P. F., & Renken, K. J. (1987). Impaction of Solid Aerosol Particles on Fine Wires. *Aerosol Science and Technology*, *7*(1), 97–107. https://doi.org/10.1080/02786828708959150

Ganguly, R., Gaind, A. P., Sen, S., & Puri, I. K. (2005). Analyzing ferrofluid transport for magnetic drug targeting. *Journal of Magnetism and Magnetic Materials*, *289*, 331–334. https://doi.org/10.1016/J.JMMM.2004.11.094

Japuntich, D. A., Stenhouse, J. I. T., & Liu, B. Y. H. (1994). Experimental results of solid monodisperse particle clogging of fibrous filters. *Journal of Aerosol Science*, *25*(2), 385–393. https://doi.org/10.1016/0021-8502(94)90089-2

Kikura, H., Takeda, Y., & Sawada, T. (1999). Velocity profile measurements of magnetic fluid flow using ultrasonic Doppler method. *Journal of Magnetism and Magnetic Materials*, *201*(1–3), 276–280. https://doi.org/10.1016/S0304-8853(99)00008-6

Niewulis, A., Podliński, J., & Mizeraczyk, J. (2009). Electrohydrodynamic flow patterns in a narrow electrostatic precipitator with longitudinal or transverse wire electrode. *Journal of Electrostatics*, *67*(2–3), 123–127. https://doi.org/10.1016/J.ELSTAT.2009.01.001

Promislow, J. H. E., & Gast, A. P. (1996). Magnetorheological Fluid Structure in a Pulsed Magnetic Field. *Langmuir*, *12*(17), 4095–4102. https://doi.org/10.1021/LA960104G

Rinaldi, C., Chaves, A., Elborai, S., He, X. (Tony), & Zahn, M. (2005). Magnetic fluid rheology and flows. *Current Opinion in Colloid & Interface Science*, *10*(3–4), 141–157. https://doi.org/10.1016/J.COCIS.2005.07.004

Ruuge, E. K., & Rusetski, A. N. (1993). Magnetic fluids as drug carriers: Targeted transport of drugs by a magnetic field. *Journal of Magnetism and Magnetic Materials*, *122*(1–3), 335–339. https://doi.org/10.1016/0304-8853(93)91104-F

Silva, C. R. N., Negrini, V. S., Aguiar, M. L., & Coury, J. R. (1999). Influence of gas velocity on cake formation and detachment. *Powder Technology*, *101*(2), 165–172. https://doi.org/10.1016/S0032-5910(98)00168-5

Song, C. B., Park, H. S., & Lee, K. W. (2006). Experimental study of filter clogging with monodisperse PSL particles. *Powder Technology*, *163*(3), 152–159. https://doi.org/10.1016/J.POWTEC.2006.01.016

Sudo, S., Asano, D., Takana, H., & Nishiyama, H. (2011). The dynamic behavior of magnetic fluid adsorbed to small permanent magnet in alternating magnetic field. *Journal of Magnetism and Magnetic Materials*, *323*(10), 1314–1318. https://doi.org/10.1016/J.JMMM.2010.11.037

Thomas, D., Penicot, P., Contal, P., Leclerc, D., & Vendel, J. (2001). Clogging of fibrous filters by solid aerosol particles Experimental and modelling study. *Chemical Engineering Science*, *56*(11), 3549–3561. https://doi.org/10.1016/S0009-2509(01)00041-0

Uehara, S., Itoga, T., & Nishiyama, H. (2015). Discharge and flow characteristics using magnetic fluid

spikes for air pollution control. *Journal of Physics D: Applied Physics*, *48*(28), 282001. https://doi.org/10.1088/0022-3727/48/28/282001

Voltairas, P. A., Fotiadis, D. I., & Michalis, L. K. (2002). Hydrodynamics of magnetic drug targeting. *Journal of Biomechanics*, *35*(6), 813–821. https://doi.org/10.1016/S0021-9290(02)00034-9

Zahn, M. (2001). Magnetic Fluid and Nanoparticle Applications to Nanotechnology. *Journal of Nanoparticle Research*, *3*(1), 73–78. https://doi.org/10.1023/A:1011497813424

Zouzou, N., Dramane, B., Moreau, E., & Touchard, G. (2011). EHD Flow and Collection Efficiency of a DBD ESP in Wire-to-Plane and Plane-to-Plane Configurations. *IEEE Transactions on Industry Applications*, *47*(1), 336–343. https://doi.org/10.1109/TIA.2010.2091473